Optica Applicata, Vol. XLV, No. 3, 2015
DOI: 10.5277/oa150305

Fiber-optic accelerometer based on a modal interferometer using a thin-core fiber

XUE WANG, XUQIANG WU*, SHILI LI, QIANG GE, TIANBO HE, BENLI YU

Key Laboratory of Opto-Electronic Information Acquisition and Manipulation of Ministry of Education, Anhui University, Jiulong Road 111#, Hefei 230601, China

*Corresponding author: atlaswoo@126.com

A compact fiber-optic accelerometer based on a modal interferometer, which is fabricated by misaligned splicing of a short section of a thin-core fiber between two sections of a standard single-mode fiber, is demonstrated experimentally. A spectrum analysis method is used to detect an acceleration signal rapidly. The experimental results show that the thin-core fiber-based fiber-optic accelerometer has a minimum detectable acceleration of $3.3\times10^{-3}g$ (g – gravitational acceleration), and a wide frequency response range from 10 to 1200 Hz. Moreover, the proposed accelerometer exhibits the advantages of low cost, simple structure and easy fabrication.

Keywords: fiber-optic accelerometer, modal interferometer, thin-core fiber.

1. Introduction

Fiber-optic sensors have found numerous sensing applications because of their distinct advantages, such as immunity to electromagnetic interference, small size and passiveness. Recently, many works have been focused on fiber modal interferometers due to their good sensing abilities and simplicity of fabrication [1–4]. In previous articles, modal interferometers based on a single-mode fiber (SMF), multimode fiber (MMF) and thin-core fiber (TCF) [5–8], have been widely adopted and applied in different fields to sense many physical parameters including curvature, displacement, strain, refractive-index, temperature and so on [9–14]. For example, LILI MAO *et al*. proposed a Mach–Zehnder interferometer (MZI) for curvature sensing and the maximum sensitivity of the structure was about –22.947 nm/m^{-1} in the range from 0.35312 to 2.8127 m^{-1} [5]. JIANGTAO ZHOU *et al*. demonstrated an intensity-modulated strain sensor based on an in-line MZI, and the strain sensor exhibited a high sensitivity of –0.023 dBm/με within a measurement range of 500 με through optical-spectral detection [10]. GUOLU YIN *et al*. reported an asymmetrical MZI for sensing a refractive-index which was realized by concatenating single-mode abrupt taper and core-offset section.

Experimental results showed that the sensitivity of the proposed sensor is 28.2 and 59.2 nm/RIU (RIU – refractive index unit) for interferometer length of 30 and 50 mm, respectively [15]. Thus, we can see that all of these works have achieved meaningful results in sensing applications. However, optical-spectral detection employed in the modal interferometers mentioned above, rather than frequency spectrum detection, were slow and costly in practical sensing applications.

In this paper, a compact fiber-optic accelerometer (FOA) based on a thin-core fiber modal interferometer is proposed. The FOA is fabricated by misaligned splicing of a short section of TCF between two sections of SMF. The whole fabrication process is quite simple and the sensor structure is cost-effective, and all optical fibers we used are single-mode fibers. As opposed to the optical-spectral detection method reported in previous papers, a spectrum detection method without any demodulation system is used in the experiment to detect the fast-changing signals.

2. Sensor design and principle

2.1. Sensor design

The configuration of the accelerometer sensing system is shown in Fig. 1. A section of TCF used as a sensing fiber is inserted between two sections of SMF to form an accelerometer sensing structure, and the sensing structure is fixed on solid frames stretched along the fiber axis. It is worth noting that the beam is only composed of a thin-core fiber as shown in Fig. 1, which is a uniform beam. The TCF-based FOA is illuminated through a tunable laser with an output power of 3.0 mW. When external acceleration makes sensing fiber deformation, the optical phase of the sensing structure will change which results in the changing of the output intensity of FOA, and then the output intensity can be observed and analyzed by signal processing circuits.

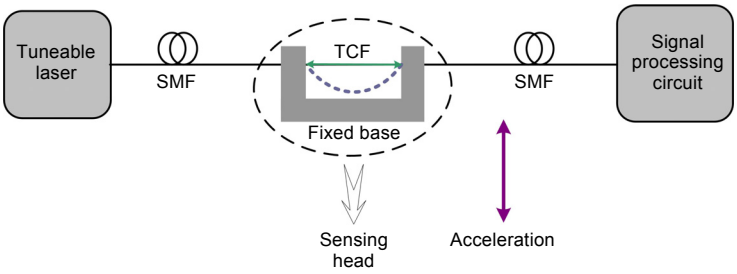

Fig. 1. Schematic diagram of the proposed TCF-based FOA.

In the experiment, the core/cladding diameters of the SMF and the TCF are 9/125 and 6.5/80 μm, respectively. In order to obtain high fringe contrast and low insertion loss, two core-offsets at spliced joints between the SMFs and the TCF are introduced. At the first misaligned splicing joint, light propagating in the lead-in fiber is divided into two parts, one propagates along the core of the TCF as a core mode, and the other propagates along the cladding of the TCF as a cladding mode. After propagating

through the TCF, the two parts of light meet and recombine in the lead-out SMF which results in modal interference. Thus, a modal interferometer based on TCF is formed.

2.2. Theoretical analyses

For modal interferometer, the optical phase difference shift between the core and cladding modes is determined by the sensing fiber length change ΔL caused by the strain effect and the difference in the effective refractive change Δn_{eff} caused by the photo-elastic effect. Because the difference in the effective refractive change Δn_{eff} is very small, we can ignore it in the experiment. So the optical phase shift induced by the vibration acceleration can be written as [13]

$$\Delta\varphi = \frac{2\pi}{\lambda}\delta n_{\text{eff}}\,\Delta L \tag{1}$$

where λ is the free-space optical wavelength in air, δn_{eff} is the difference in the effective refractive indices between the core and the cladding modes.

A simple analytical model shown in Fig. 2 is used to calculate the sensitivity and the resonant frequency of the accelerometer.

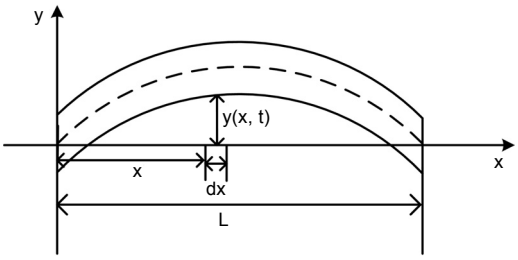

Fig. 2. Analytical model of the sensing structure.

According to [16, 17], the sensing fiber length change ΔL can be calculated as

$$\Delta L = \frac{mdL^2}{24EI}\,a \tag{2}$$

where E is the Young's modulus of the fiber, I represents the inertia moment, d is the cladding diameter of the thin-core fiber, L is the length of the sensing fiber, m is the mass of the fiber beam, and a is the vibration acceleration.

Inserting Eq. (2) into Eq. (1), the phase shift can be expressed as

$$\Delta\varphi = \frac{\pi\,\delta n_{\text{eff}}\,dL^2}{12\lambda EI}\,ma \tag{3}$$

Assuming interferometer operates in the linear region by tuning optical wavelength without any acceleration excitation. When acceleration excitation is applied to the FOA, considering the phase shifts are very small near the linear operating point, the corre-

sponding voltage change can be regarded as linear. Thus, the output voltage can be considered as proportional to the phase shifts of the interference output. It can be expressed as

$$V_{\text{out}} = \zeta R_0 I_0 (1 + v k_Q \varphi) \tag{4}$$

where ζ and R_0 are the response factor and conversion resistance of a photodiode (PD) detector, respectively, I_0 is the corresponding light intensity of the quadrature point, v is the visibility of the interference, and k_Q is the slope at the quadrature point.

According to Eqs. (3) and (4), the acceleration sensitivity can be written as

$$\frac{\Delta V_{\text{out}}}{a} = \zeta R_0 I_0 k_Q v \frac{\pi \delta n_{\text{eff}} dL^2}{12 \lambda EI} m \tag{5}$$

By the Newton's second law, the differential equation of motion of the transverse vibration of the beam can be given by [18]

$$EI \frac{\partial^4 y}{\partial x^4} + m \frac{\partial^2 y}{\partial t^2} = 0 \tag{6}$$

For the uniform beam structure, its boundary conditions can be given as

$$\left.\begin{aligned} y|_{x=0} &= 0, \quad \left.\frac{\mathrm{d}y(x)}{\mathrm{d}x}\right|_{x=0} = 0 \\ y|_{x=L} &= 0, \quad \left.\frac{\mathrm{d}y(x)}{\mathrm{d}x}\right|_{x=L} = 0 \end{aligned}\right\} \tag{7}$$

According to Eqs. (6) and (7), the fundamental frequency of the simple supported beam structure can be given by

$$f = \frac{\pi^2}{L^2} \sqrt{\frac{EI}{\rho A}} \tag{8}$$

where ρ is the density of the fiber, and A is the cross-sectional area of the TCF.

3. Experimental details and discussions

In the splicing process, an erbium-doped fiber amplified spontaneous emission (ASE) light source and an AQ6370C optical spectrum analyzer (OSA) are used to acquire the interference spectrum. The core-offset values are 3.0 and 4.5 μm, respectively. The transmission spectrum of the proposed interferometer is shown in Fig. 3. From this figure, we can see that the interference spectrum is uniform and the fringe contrast is about 13 dB. And the inset of Fig. 3 is ASE spectrum which constitutes the envelope of an interference pattern.

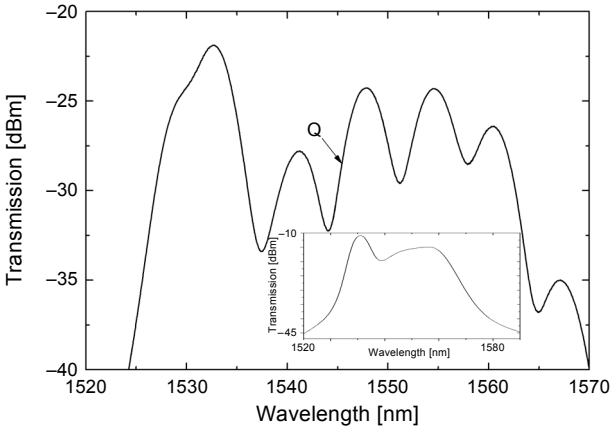

Fig. 3. Interference fringe pattern of the FOA.

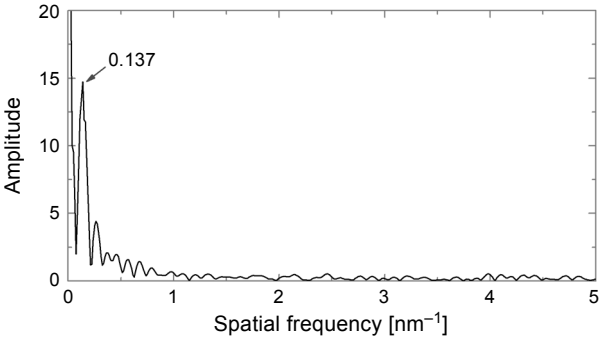

Fig. 4. Spatial frequency spectrum of the proposed interferometer.

To confirm the number and power distribution of the interference modes, the wavelength spectrum in Fig. 3 is Fourier transformed to get the spatial frequency of the interference fringe; the result is shown in Fig. 4. Following the analysis in [19], the relationship between the spatial frequency and the interferometer length can be given as

$$\xi = \frac{\delta n_{\text{eff}}}{\lambda^2} L \tag{9}$$

As shown in Fig. 4, we can see that there is indeed one dominant spatial frequency corresponding to an interference fringe (point 0.137 nm^{-1}), along with other weakly excited ones. According to Eq. (9), δn_{eff} can be calculated as 0.013.

In order to investigate the performance of the TCF-based FOA, proof-of-principle experiments are carried out, a test system for measuring the vibration acceleration is shown in Fig. 5. It is worth mentioning that all of experimental equipments are placed on a vibration insulation table to prevent the interference of environment. Besides, this

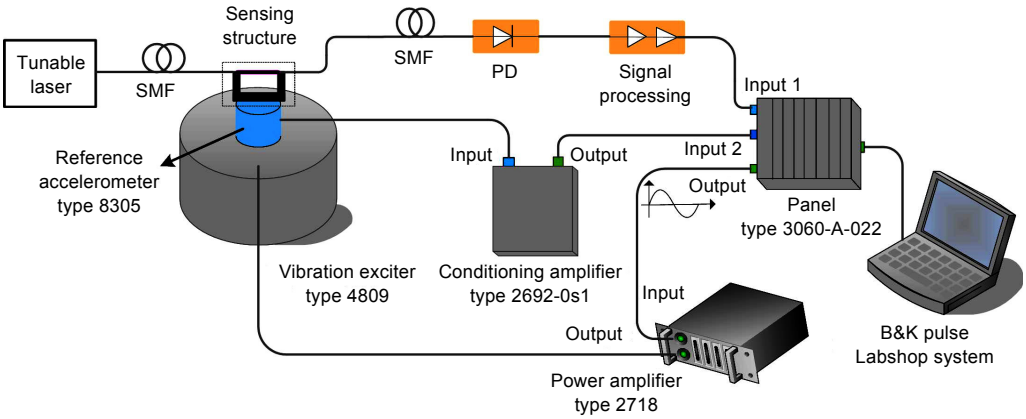

Fig. 5. Test system of the fiber-optic accelerometer.

experiment is carried out at room temperature, so the influence of temperature can be ignored. The FOA structure is horizontally mounted on a reference accelerometer (RA, B&K 8305), and the RA is vertically mounted on a vibration exciter (B&K 4809). A signal generator (B&K 3160-A-022) and a power amplifier (B&K 2178) are used to drive the vibration exciter. The received optical signal is detected by signal processing circuits, and then analyzed in B&K Pulse Labshop system installed in PC. The experiments include a sensitivity test and an amplitude-frequency characteristic test.

In the experiment, the sensing fiber length is 2.70 cm, and there is no loading mass on the sensing fiber. Figure 6 shows the relationship between the output voltage and acceleration when the vibration frequency is 80 Hz. We can observe that the acceleration and the output voltage show a linear relationship. The voltage sensitivity of the accelerometer is 1.54 mV/g (g is gravitational acceleration), and the linearity is 0.9978. The inset of Fig. 6 shows the spectral response of the accelerometer when

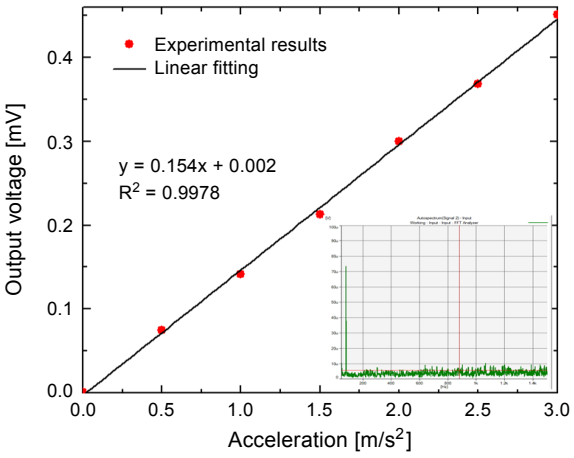

Fig. 6. Relationship between the output voltage and acceleration.

the vibration frequency is 80 Hz. We can see that the background noise is about 5 μV, and it is stable and almost no electromagnetic interference and environmental interference can be observed. Therefore, the minimum detectable acceleration is $3.3\times10^{-3}g$.

The resonant frequency of the TCF-based FOA is also measured for getting its working bandwidth. The sine excitation frequency is gradually increased to 2000 Hz when acceleration remains unchanged at $0.02g$ by changing the amplitude of the excitation signal. In order to determine the frequency response range, the B&K Pulse Labshop system installed on PC is used to obtain the output voltage of every frequency, and the vibration exciter of B&K 4809 covers the frequency range from 10 Hz to 12.8 kHz. The amplitude-frequency characteristic is shown in Fig. 7; we can observe that the resonant frequency is 1451 Hz and the available bandwidth of the fiber-optic accelerometer range is from 10 to 1200 Hz.

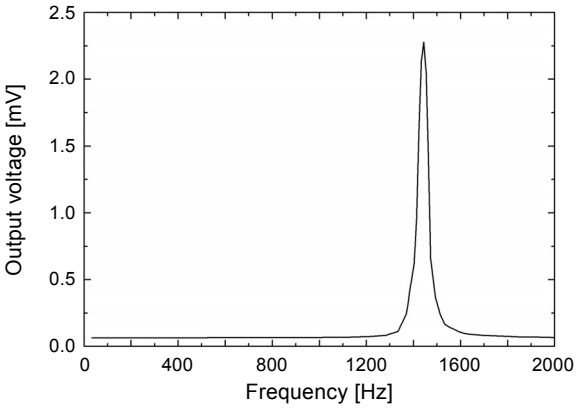

Fig. 7. Amplitude-frequency characteristic of the accelerometer.

In the experiment, $\zeta = 0.95$ mA/mW, $R_0 = 1$ kΩ, $I_0 = 0.58$ mW, $\lambda = 1550$ nm, $E = 7.2\times10^{10}$ N/m^2, $d = 80$ μm, $I = \pi d^4/64$, $A = \pi d^2/4$, $L = 2.70$ cm, $\rho = 2.3\times10^3$ kg/m^3, $\delta n_{\text{eff}} = 0.013$. For two-beam interference, the slope k_Q at the quadrature point and the visibility of the fringe pattern v can be considered as 1. Using Eqs. (5) and (8), we can calculate that the theoretical acceleration sensitivity and resonance frequency are 1.60 mV/g and 1490 Hz, respectively. Compared with the experimental results, the experimental errors are within 5%. Consequently, the experimental results are consistent with the theoretical analyses. And the experimental results indicate the feasibility of the fiber-optic accelerometer system for acceleration measurement. According to Eqs. (5) and (8), the Young's modulus E, the inertia moment I, the sensing length L, and the sensing fiber mass m have an impact on the acceleration sensitivity and the resonant frequency. And any of these parameters can affect the acceleration sensitivity and the resonant frequency. Moreover, the sensing length L is the easiest adjustable and most sensitive parameter for changing the acceleration sensitivity and the resonant frequency, so we can optimize the performance of the accelerometer by adjusting the length of the sensing fiber in practical applications. In fact, the performance of

fiber-optic acceleration can also be improved by adding a loading mass on the sensing fiber in further experiments.

4. Conclusions

In summary, a compact fiber-optic accelerometer system based on a thin-core fiber modal interferometer is demonstrated. Frequency spectrum detection is used in the paper to replace the optical-spectral detection, which is simple and fast in practical applications. The experimental results show that the accelerometer has a minimum detectable acceleration of $3.3\times10^{-3}g$ and the frequency response range of 1200 Hz. Besides, the performance of the fiber-optic accelerometer can be improved by adjusting the length of the sensing fiber or adding a loading mass on the sensing fiber. The experimental result indicates the feasibility of the fiber-optic accelerometer system for acceleration measurement. Moreover, the fiber-optic accelerometer proposed in the article exhibits many competitive advantages including low cost, easy fabrication and compactness.

Acknowledgements – This work was supported by two found projects named Key Research Project of Anhui Education Department (No. KJ2010A033) and Research Fund for the Doctoral Program of Higher Education of China (No. 201223401120012). Here we deeply appreciate the supporter for offering the found projects.

References

[1] ZHIGANG CAO, XIAOCHUN JI, RUI WANG, ZHAO ZHANG, TAO SHUI, FENG XU, BENLI YU, *Compact fiber sensor with high spatial resolution for simultaneous strain and temperature measurement*, IEEE Sensors Journal **13**(5), 2013, pp. 1447–1451.

[2] QIAN WANG, FARRELL G., WEI YAN, *Investigation on single-mode–multimode–single-mode fiber structure*, Journal of Lightwave Technology **26**(5), 2008, pp. 512–519.

[3] YIZHENG ZHU, ANBO WANG, *Miniature fiber-optic pressure sensor*, IEEE Photonics Technology Letters **17**(2), 2005, pp. 447–449.

[4] ZHAOBING TIAN, YAM S.S.-H., *In-line single-mode optical fiber interferometric refractive index sensors*, Journal of Lightwave Technology **27**(13), 2009, pp. 2296–2306.

[5] LILI MAO, PING LU, ZEFENG LAO, DEMING LIU, JIANGSHAN ZHANG, *Highly sensitive curvature sensor based on single-mode fiber using core-offset splicing*, Optics and Laser Technology **57**, 2014, pp. 39–43.

[6] PENGFEI WANG, BRAMBILLA G., MING DING, SEMENOVA Y., QIANG WU, FARRELL G., *Investigation of single-mode–multimode–single-mode and single-mode–tapered-multimode–single-mode fiber structures and their application for refractive index sensing*, Journal of the Optical Society of America B **28**(5), 2011, pp. 1180–1186.

[7] JIANGTAO ZHOU, CHANGRUI LIAO, YIPING WANG, GUOLU YIN, XIAOYONG ZHONG, KAIMING YANG, BING SUN, GUANJUN WANG, ZHENYONG LI, *Simultaneous measurement of strain and temperature by employing fiber Mach–Zehnder interferometer*, Optics Express **22**(2), 2014, pp. 1680–1686.

[8] JING-JING ZHU, ZHANG A.P., TIAN-HAO XIA, SAILING HE, WEI XUE, *Fiber-optic high-temperature sensor based on thin-core fiber modal interferometer*, IEEE Sensors Journal **10**(9), 2010 pp. 1415–1418.

[9] MEHTA A., MOHAMMED W., JOHNSON E.G., *Multimode interference-based fiber-optic displacement sensor*, IEEE Photonics Technology Letters **15**(8), 2003, pp. 1129–1131.

[10] JIANGTAO ZHOU, YIPING WANG, CHANGRUI LIAO, GUOLU YIN, XI XU, KAIMING YANG, XIAOYONG ZHONG, QIAO WANG, ZHENGYONG LI, *Intensity-modulated strain sensors based on fiber in-line Mach–Zehnder interferometer*, IEEE Photonics Technology Letters **26**(5), 2014, pp. 508–511.

[11] JIANFENG WANG, YONGXING JIN, YU ZHAO, XINYONG DONG, *Refractive index sensor based on all-fiber multimode interference*, Optik – International Journal for Light and Electron Optics **124**(14), 2013, pp. 1845–1848.

[12] TIAN-HAO XIA, A. PING ZHANG, BOBO GU, JING-JING ZHU, *Fiber-optic refractive-index sensors based on transmissive and reflective thin-core fiber modal interferometers*, Optics Communications **283**(10), 2010, pp. 2136–2139.

[13] DE-WEN DUAN, YUN-JIANG RAO, LAI-CAI XU, TAO ZHU, MING DENG, DI WU, JUN YAO, *In-fiber Fabry–Perot and Mach–Zehnder interferometers based on hollow optical fiber fabricated by arc fusion splicing with small lateral offsets*, Optics Communications **284**(22), 2011, pp. 5311–5314.

[14] YUJUAN ZHANG, LINLIN XUE, TONGXIN WANG, LI YANG, BING ZHU, QIJIN ZHANG, *High performance temperature sensing of single mode–multimode–single mode fiber with thermo-optic polymer as cladding of multimode fiber segment*, IEEE Sensors Journal **14**(4), 2014, pp. 1143–1147.

[15] GUOLU YIN, SHUQIN LOU, HUI ZOU, *Refractive index sensor with asymmetrical fiber Mach–Zehnder interferometer based on concatenating single-mode abrupt taper and core-offset section*, Optics and Laser Technology **45**, 2013, pp. 294–300.

[16] BUDYNAS R.G., *Advanced Strength and Applied Stress Analysis*, 2nd Ed., McGraw-Hill, 1999, pp. 849–857.

[17] FENG PENG, JUN YANG, BING WU, YONGGUI YUAN, XINGLIANG LI, AI ZHOU, LIBO YUAN, *Compact fiber optic accelerometer*, Chinese Optics Letters **10**(1), 2012, article 011201.

[18] XIJUN LIU, QIFEN JIA, WENDE ZHANG, *Engineering Vibration and Testing Techniques*, Tianjin University, 1999, pp. 118–121.

[19] HAE YOUNG CHOI, MYOUNG JIN KIM, BYEONG HA LEE, *All-fiber Mach–Zehnder type interferometers formed in photonic crystal fiber*, Optics Express **15**(9), 2007, pp. 5711–5720.

Received March 22, 2015
in revised form April 26, 2015